Supplementary Materials

Supplementary Methods

Person Recognition Task

Participants ($N_{participants}$ = 14, $n_{sessions}$ = 40) were instructed to learn a series of 16-56 images of novel people [1] presented serially on a computer screen for 4 s each and preceded by a jittered interval of 4-4.5s. Stimulation was applied for a period of 1 s, between 2.2 and 2.7 s prior to a randomly selected half of stimuli. This encoding period was followed by a 30-second odd/even distractor task. During the retrieval stage, a randomly shuffled image set of previously seen photographs ("Targets") and similar-looking photographs ("Lures") were presented for 4 s each, and participants were given up to 16 s to rate whether the images were "new" or "old" and then rated their confidence on a continuous scale from -100 ("not confident") to 100 ("very confident") (Fig. S3A). The fraction of remembered images were calculated as described for the object recognition task. A subset of data from this task (13/14 participants and 38/40 sessions) were published previously [2].

Object Recognition Task

During the encoding stage, participants ($N_{participants}$ = 9, $n_{sessions}$ = 36) were presented with a series of 30-46 images depicting everyday objects that were downloaded from Google Image Search and the Hemera Object Database [3]. Nineteen undergraduate students from the UCLA Psychology Department Subject Pool completed the task, and the top and bottom 10% of rated objects were removed from the stimulus database to achieve suitable task difficulty level. To promote task engagement, participants were instructed to determine whether each presented object was "bigger or smaller than a shoebox" and to answer by key press. Images were shown for 4 s and interleaved with jittered fixation periods of 4-4.6 s. Stimulation was applied for 3 s, beginning 3 s prior to a randomly selected half of stimuli and terminating before stimulus onset (In 2 sessions, stimulation duration was only 1 s). Participants then

completed the 30-second odd/even distractor task. For each image shown during encoding, three images were shown, in random order, during the retrieval stage. These included the original image ("Target"), a very similar image ("Lure"), and a dissimilar image from the same object category ("Foil"). Participants were given up to 60 s to rate each image (each trial terminated with the participant's response) on a six-point confidence scale, where "1," "2," and "3" indicated that the image was "new" (not seen during encoding) and "4," "5," and "6" indicated that the image was "old" (already viewed). Ratings of "1" and "6" indicated high confidence ("definitely"), "2" and "5" indicated medium confidence ("probably"), and "3" and "4" indicated low confidence ("maybe") (Fig. S3B). Performance on this task was measured by the fraction of remembered images, defined as targets that were correctly categorized as old whose corresponding lure was correctly categorized as new.

Face-Name Associative Memory Task

Participants ($N_{participants} = 6$, $n_{sessions} = 11$) were presented with a series of either 16 or 32 novel face-name pairs and instructed to learn each pairing. Each face-name pair was shown for 4 s, interleaved with fixation periods of the same duration. Stimulation was applied for 3 s, beginning 3 s prior to a randomly selected half of stimuli. Following the 30-second odd/even distractor task, each image shown during the encoding stage was presented again, in random order. Participants were given 4 s to recall the name associated with each image. For participants with especially poor memory (1 participant; 3 sessions), the first letter of the name was presented as a cue during retrieval. After the retrieval phase, the experiment began again with the encoding phase, using the same set of images (with the same subset of images receiving stimulation) to give participants another opportunity to learn the associations. In total, participants saw each set of images six times (data were excluded if fewer than 6 blocks were completed). For each block, memory performance was calculated as the percentage of correctly identified names for stimulated and non-stimulated trials. Because we wanted to test the end result of

learning with or without stimulation, only the scores for the sixth block were included in the model (Fig. S3C).

Details of Electrode Localization Method

Methods for determining the location of the stimulating electrodes were as described previously [2]. Briefly, a high-resolution post-operative computed tomography (CT) scan was co-registered (Fig. S1) to a pre-operative whole brain magnetic resonance imaging (MRI, TR 11 ms; TE 2.81 ms; flip angle 20 degrees; matrix size 256 × 256 mm; FOV 256 mm; in-plane resolution 1 × 1 mm; slice thickness 1 mm; voxel size 1 mm isotropic) and high-resolution MRI (TR: 5300 ms; TE: 70 ms; flip angle: 178 degrees; matrix size: 500 × 500 mm; FOV: 200 mm; in-plane resolution: 0.4 × 0.4 mm; slice thickness: 3 mm, voxel size: 0.4 × 0.4 x 3 mm, 19 slices, Fig. 2) using BrainLab (Westchester, IL) stereo-tactic and localization software (www.brainlab.com) [4, 5] and FSL FLIRT (FMRIB's Linear Registration Tool) [6, 7]. Bipolar macro- and micro-electrode contacts were manually delineated using visualization and tools in BrainLab. Since only the tip of the entire bundle of 8 micro-electrodes is visible in BrainLab, the tip of the micro-stimulation electrode was estimated by measuring 2 mm from the tip of the bundle to the first (most distal) macro-electrode contact. A much larger red crosshair (2 mm wide × 2 mm long, Fig. 2) was then used as a conservative estimate to represent the area in which the micro-stimulation electrode tip (100 μm diameter) was located. One participant was excluded due to the proximity of their electrode being too close to the white/gray matter boundary. Medial temporal lobe regions (entorhinal, perirhinal, parahippocampal, and hippocampal subfields CA23DG [CA2, CA3, dentate gyrus], CA1, and subiculum) were delineated using the Automatic Segmentation of Hippocampal Subfields (ASHS [8, 9]) software using boundaries determined from MRI visible landmarks that correlate with underlying cellular histology (Fig.1, S2) [10, 11]. White matter and cerebral spinal fluid areas were outlined using FSL FAST software [12]. Together, similar methods have been previously used to localize micro-

electrodes and investigate structural and functional dissociations within human medial temporal lobe subregions [13-15]. Each electrode contained macro-electrodes, spaced at 1.5 mm (3.5 mm center to center) intervals along the shaft (most distal 2 contacts were used for macro-stimulation), a single 100-µm micro-electrode (used for micro-stimulation) at the distal tip 3 mm from the most distal macro-contact, and a bundle of seven 40-µm micro-electrodes (not used for stimulation) 5 mm from the most distal macro-contact. Macro- and micro-electrode contacts were identified and outlined on the post-operative CT scan. To determine whether each micro- or macro-electrode fell within white or gray matter, the high-resolution MRI, with ASHS and FAST segmentation results, was overlaid with the co-registered electrode. At minimum, if the more distal of the two stimulating macro-electrodes fell within the white matter (angular bundle) region, it was classified as "white." The co-registered CT electrode locations and high-resolution MRIs of example participants are shown in Fig. S2. Table S3 includes additional information—both the localization result for each electrode contact as well as the corresponding clinical label.

Brain Imaging Parameters

MRI data were acquired on a Siemens Magnetom Prisma 3 Tesla system housed in the Department of Radiology at UCLA. The whole brain MRI images were collected over 176 axial slices using a T1-weighted gradient echo sequence (TR = 11 ms; TE = 2.81 ms; flip angle = 20 degrees; matrix size = 256 x 256 mm; FOV = 256 mm; in-plane resolution = 1 x 1 mm; slice thickness 1 mm; voxel size = 1 mm isotropic). A high-resolution T2 weighted structural scan was also acquired for each participant (TR = 5300 ms; TE = 70 ms; flip angle = 178 degrees; matrix size = 500 x 500 mm; FOV = 200 mm; in-plane resolution = 0.4 x 0.4 mm; slice thickness = 3 mm, voxel size = 0.4 x 0.4 x 3 mm, 19 slices).

Spiral computed CT scans were performed on a 64-row multi-detector CT scanner. All scans had a pre-contrast series and single phase, post-contrast acquisition, synchronized using bolus tracking technique

for arterial phase. Omnipaque 350 contrast media volume was set as 100 cc with an infusion rate of 3.0 cc/s.

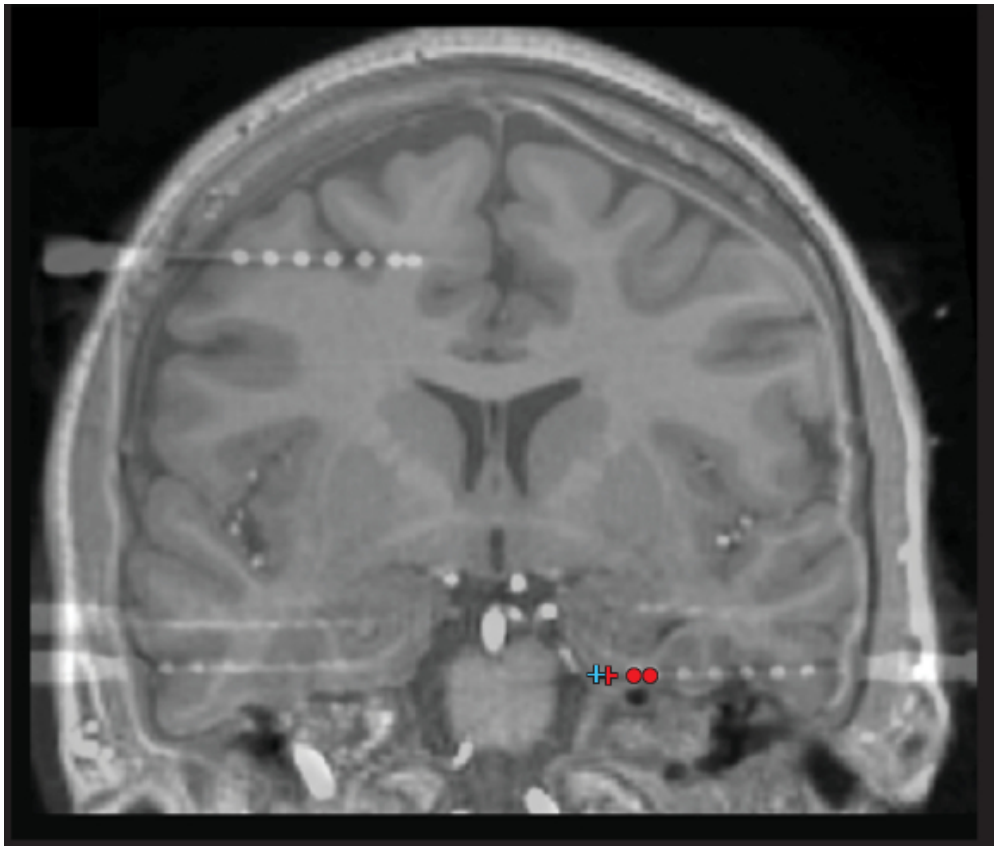

Fig. S1. Co-registered MRI and CT scan. Example co-registration of a high-resolution T2 MRI overlaid onto a corresponding high-resolution CT. Macro-electrodes are shown as red dots, while micro-electrode locations are presented as red (stimulating electrode) or blue (recording electrodes) crosshairs.

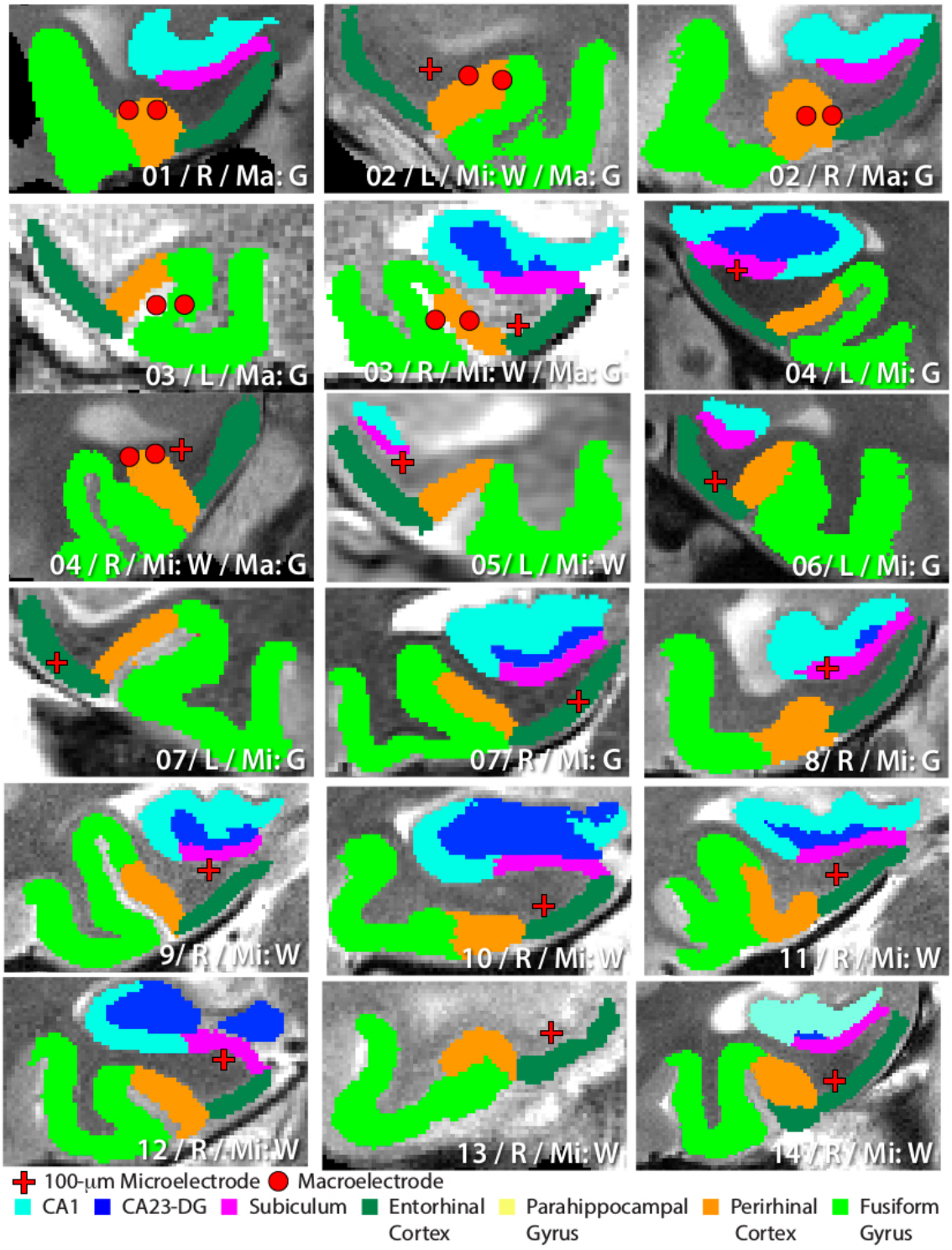
01 / R / Ma: G
02 / L / Mi: W / Ma: G
02 / R / Ma: G
03 / L / Ma: G
03 / R / Mi: W / Ma: G
04 / L / Mi: G
04 / R / Mi: W / Ma: G
05/ L / Mi: W
06/ L / Mi: G
07/ L / Mi: G
07/ R / Mi: G
8/ R / Mi: G
9/ R / Mi: W
10 / R / Mi: W
11 / R / Mi: W
12 / R / Mi: W
13 / R / Mi: W
14 / R / Mi: W
100-μm Microelectrode
Macroelectrode
CA1
CA23-DG
Subiculum
Entorhinal Cortex
Parahippocampal Gyrus
Perirhinal Cortex
Fusiform Gyrus

106

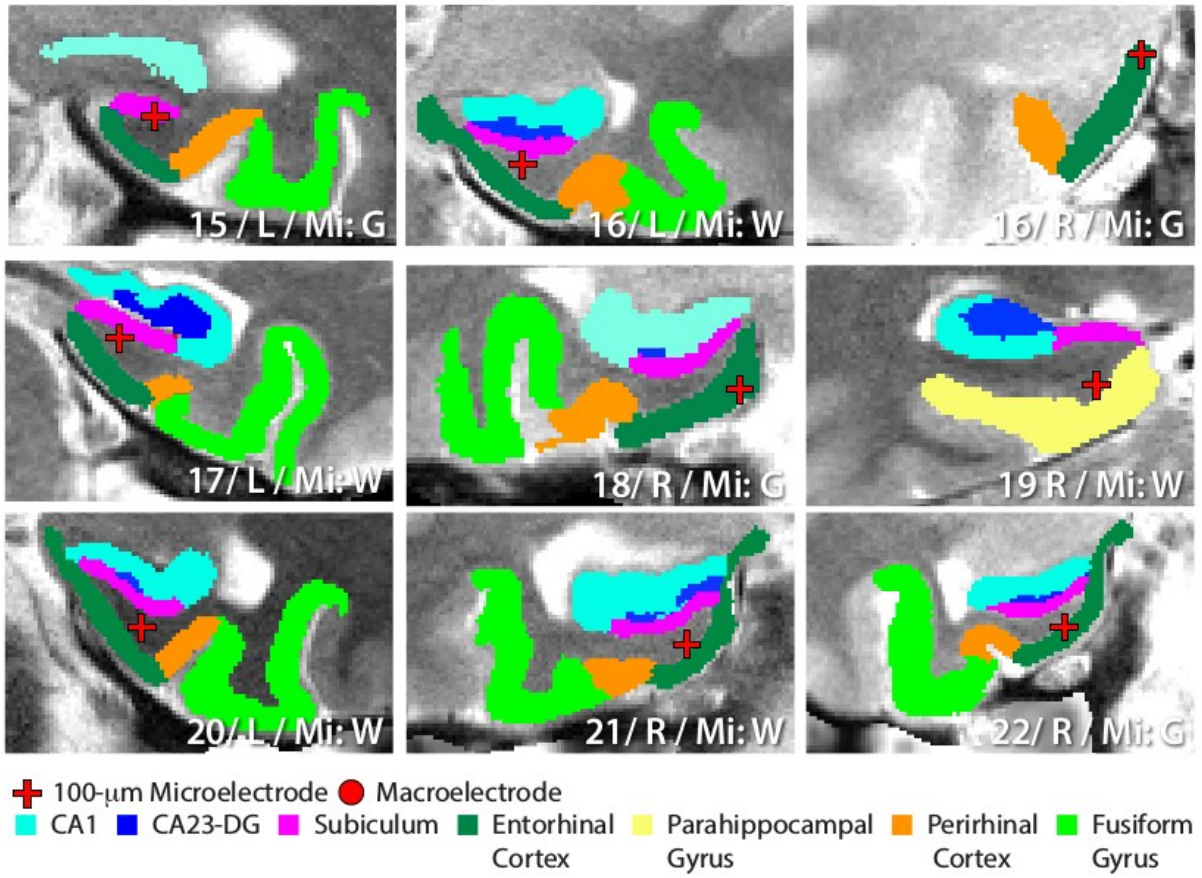

Fig. S2. Electrode localizations for each study participant

Electrode localizations for each study participant are labeled with corresponding *participant (#) / hemisphere (left [L] or right [R]) / electrode placement (micro [Mi.] and/or macro [Ma.] in white [W] or gray [G] matter)*.

115

Demographics and Clinical Characteristics of Participants								
Participant ID	**Age**	**Handedness**	**Verbal IQ**	**Digit Span**	**Verbal Memory**		**Visual Memory**	**Executive Function**
					WMS	*CVLT*		
1	51	R	90 [a]	16	63	21 [c]	< 1	27
2	20	R	108	16	37	69	2	46
3	40	R	98	16	2	1	5 [d]	5
4	45	A	85	12	25	< 1 [c]	< 1	< 1
5	34	R	85	8.1	< 1	< 1	< 1	63
6	35	L	105	37	50	50	7	63
7	30	A	134	37	63	50	96	92
8	27	R	98	37	16	7	9 [d]	16
9	20	R	102	37	50	50	12	63
10	26	R	83 [f]	-	61 [e]	8 [e]	22	-
11	21	R	95	9	37	2	8	21
12	49	R	120	25	75	50	16	10
13	35	R	91	9	16	69	14	16
14	28	R	96	16	25 [b]	69	< 1 [d]	27
15	27	R	89	9	-	16	-	-
16	33	R	107	63	91	94	66	92
17	47	R	112	63	5	4[c]	16 [d]	56
18	53	R	75	16	9	1	12 [d]	1
19	29	R	-	-	-	-	-	-
20	44	R	-	50	99.6	16	82	32
21	47	A	87	37	16	16	< 1	16
22	21	R	-	-	-	-	-	-

116 **Table S1. Clinical characteristics of the study participants**.

117 Except as noted, Verbal and digit span (i.e., attention) were calculated with the use of the
118 Wechsler Adult Intelligence Scale [16], verbal memory by means of the verbal paired associates
119 delayed recall portion of the Wechsler Memory Scale (WMS) [16] and the long-delay free-recall
120 portion of the California Verbal Learning Test (CVLT) [17], visual memory with the use of the
121 30-minute delayed version of the Rey–Osterrieth Complex Figure Test [18] and executive
122 function by means of the Trail Making Test, Part B [19]. Except for Verbal IQ, all scores are
123 given as percentiles.

[a]Full Scale IQ; [b]Logical Memory Delayed Recall; [c]Rey Auditory Verbal Learning Test score; [d]3-minute delayed version of the Rey-Osterreith Complex Figures Test; [e]Spanish Neuropsychological Exam Equivalent Version; [f]Wide Range Achievement Test Spelling Score, [g]Woodcock-Johnson III

Participant	Macro-stimulation				Micro-stimulation				Seizure Onset Area
	Left Entorhinal		Right Entorhinal		Left Entorhinal		Right Entorhinal		
	White	Gray	White	Gray	White	Gray	White	Gray	
1				(X)*					Bilateral Temporal
2		X*		X*	X				Extra-Temporal
3		X*		(X)*†			(X)†		Right Medial Temporal
4				X*		(X)*†	X*		Left Medial Temporal
5					X*†				Right Medial Temporal
6						X			Extra-Temporal
7						X*		(X)*	Right Medial Temporal
8								(X)	Right Medial Temporal
9							X*		Left Medial Temporal
10							X*		Extra-Temporal
11							X		Left Anterior Temporal
12							X		Left Medial Temporal
13							X		Left Medial Temporal
14							X*		Bilateral Temporal
15						X*			Right Temporal
16					X*			X*	Right Medial Frontal
17					(X)				Left Medial Temporal
18								(X)*	L/R Medial Temporal
19							(X) *		L/R Medial Temporal
20					(X)*				L/R Medial Temporal
21							(X) *†		L/R Medial Temporal
22								X*	Left Temporal and ExtraTemporal

Table S2. Localization Details of Electrodes Used in the Study

White or gray matter placements of entorhinal depth macro- and micro-electrodes for all participants, as well as epileptogenic onset areas determined by clinical evaluation. Note that a macro electrode pair was considered to be in white matter if at least the most distal of the bipolar macro-electrode contacts was fully in white matter. A red (X) denotes an electrode that fell within an area that was later determined to be epileptogenic. *Anti-epileptic drug(s) were administered to participant within 24 hours of stimulation session at given electrode at least once. †The associated hemisphere was diagnosed with mesial temporal sclerosis.

Participant	Electrode Label	Electrode Type	Localization (Contact 1)	Localization (Contact 2)
1	REC	Macro	Perirhinal Cortex	Perirhinal Cortex
2	LEC	Macro	Perirhinal Cortex	Perirhinal Cortex
2	REC	Macro	Perirhinal Cortex	Fusiform Gyrus
3	REC	Macro	Perirhinal Cortex	Fusiform Gyrus
3	LEC	Macro	Perirhinal Cortex	Fusiform Gyrus
4	REC	Macro	Hippocampus (Subiculum)	Hippocampus (Subiculum)
4	LEC	Micro	Entorhinal Cortex	N/A
6	LEC	Micro	Entorhinal Cortex	N/A
7	REC	Micro	Entorhinal Cortex	N/A
7	LEC	Micro	Entorhinal Cortex	N/A
8	REC	Micro	Hippocampus (Subiculum)	N/A
15	LEC	Micro	Subiculum	N/A
16	REC	Micro	Entorhinal Cortex	N/A
18	REC	Micro	Entorhinal Cortex	N/A
22	REC	Micro	Entorhinal Cortex	N/A

Table S3. Specific Localization Details of Electrodes not localized to Entorhinal White Matter. 15 stimulating micro-electrodes or macro-electrode pairs fell within gray matter of the medial temporal subregions. Electrode clinical labels include right entorhinal cortex (REC) and left entorhinal cortex

(LEC). However, for each stimulated macro-electrode pair (contact 1 is more distal than contact 2) or micro-electrode, contacts were in fact localized to entorhinal cortex (more inferior medial placements), perirhinal cortex (more lateral inferior placement), or hippocampal subiculum (more superior placement). Micro-electrode contacts (both stimulating and reference electrode) are localized to the same region (contact 1) and therefore localization of contact 2 is not applicable (N/A). All white matter stimulating electrodes were localized to the angular bundle (Participant 19 to parahippocampal white matter; all others to entorhinal white matter, both of which are known to contain perforant pathway fibers [20]).

Participant	Memory Task	White/Gray	Left/Right	Macro/Micro
1	Face-Name	Gray	Right	Macro
2	Face-Name	Gray	Right	Macro
	Object	Gray	Left	Macro
	Object	White	Left	Micro
	Person	White	Left	Micro
3	Face-Name	White	Right	Micro
	Face-Name	Gray	Right	Macro
	Face-Name	Gray	Left	Macro
	Person	White	Right	Micro
4	Face-Name	White	Right	Micro
	Face-Name	Gray	Left	Micro
	Object	Gray	Right	Macro
	Object	Gray	Left	Micro
	Object	White	Right	Micro
	Person	Gray	Left	Micro
5	Object	White	Left	Micro
	Person	White	Left	Micro
6	Person	Gray	Left	Micro
7	Person	Gray	Left	Micro
	Person	Gray	Right	Micro
8	Person	Gray	Right	Micro
9	Person	White	Right	Micro
10	Person	White	Right	Micro
11	Object	White	Right	Micro
12	Person	White	Right	Micro

13	Person	White	Right	Micro
14	Person	White	Right	Micro
15	Person	Gray	Left	Micro
16	Person Person	Gray White	Right Left	Micro Micro
17	Object	White	Left	Micro
18	Object	Gray	Right	Micro
19	Face-Name	White	Right	Micro
20	Face-Name Object	White White	Left Left	Micro Micro
21	Object	White	Right	Micro
22	Object	Gray	Right	Micro

Table S4. Summary of experiments in each participant. Shown is the type of memory task completed by each participant and the region of stimulation (white/gray, left/right hemisphere, and macro/micro-stimulation). All macro-stimulation sessions used the following parameters: 50 Hz (frequency), 300 μsec (pulse width), 0.4 – 6 mA (current amplitude, depending on the after-discharge threshold, see Methods). All micro-stimulation sessions used a theta-burst protocol: one waveform of 4-pulses at 100 Hz (frequency), 200 μsec (pulse width), 100 μsec (inter-pulse interval), 150 μA (current amplitude), repeated every 200 msec. Stimulation duration was 3 sec for object recognition and face-name associative memory and 1 sec for person recognition.

Data file S1. All data used in the manuscript. This file contains data for each experimental session included in the analysis. Each row contains the following information: ParticipantID is a numerical tag for each participant; SessionNum is greater than one if a participant completed the same task more than once. BlockNumber indicates the block within a single experimental session. For Person Recognition and Object Recognition, BlockNumber is always 1, because stimuli were not repeated. For Face Name Associative Memory, Block Number increases from 1 to 6 within each Session Number. To assess the effect of stimulation at the end of learning, only Block 6 was included in analysis. White is 1 if the stimulating electrode was localized to white matter and 0 otherwise. Right is 1 if the stimulating

electrode was in the right hemisphere and 0 otherwise. Macro is 1 if the stimulating electrode was a pair of macro electrodes and 0 if it was a micro electrode. BehavioralTask is the name of the task completed, and BehTaskNum is a numerical code for the same variable. DifferenceScore is the main measure analyzed and indicates the fraction difference between memory of stimulated and non-stimulated items (positive numbers indicate better performance on stimulated items).

Source code S1. SPSS Syntax file for completing analysis. All analysis was completed in SPSS. After opening Data file S1, the syntax file will produce relevant SPSS output.

References (Supplementary Material Section Only)

[1] Versluis A, Uyttenbroek E. Exactitudes. 1st ed.: nai010 Publishers; 2002.

[2] Titiz AS, Hill MRH, Mankin EA, Aghajan ZM, Eliashiv D, Tchemodanov N, et al. Theta-burst microstimulation in the human entorhinal area improves memory specificity. Elife 2017;6. https://doi.org/10.7554/eLife.29515

[3] Brady TF, Konkle T, Alvarez GA, Oliva A. Visual long-term memory has a massive storage capacity for object details. Proceedings of the National Academy of Sciences 2008;105(38):14325. https://doi.org/10.1073/pnas.0803390105

[4] Gumprecht HK, Widenka DC, Lumenta CB. BrainLab VectorVision Neuronavigation System: technology and clinical experiences in 131 cases. Neurosurgery 1999;44(1):97-104; discussion -5. https://doi.org/10.1097/00006123-199901000-00056

[5] Schlaier J, Warnat J, Dorenbeck U, Proescholdt M, Schebesch K-M, Brawanski A. Image fusion of MR images and real-time ultrasonography: evaluation of fusion accuracy combining two commercial instruments, a neuronavigation system and a ultrasound system. Acta Neurochir (Wien) 2004;146(3):271-7. https://doi.org/10.1007/s00701-003-0155-6

[6] Jenkinson M, Bannister P, Brady M, Smith S. Improved optimization for the robust and accurate linear registration and motion correction of brain images. Neuroimage 2002;17(2):825-41.

[7] Jenkinson M, Smith S. A global optimisation method for robust affine registration of brain images. Med Image Anal 2001;5(2):143-56. https://doi.org/10.1016/s1361-8415(01)00036-6

[8] Pluta J, Yushkevich P, Das S, Wolk D. In vivo analysis of hippocampal subfield atrophy in mild cognitive impairment via semi-automatic segmentation of T2-weighted MRI. J Alzheimers Dis 2012;31(1):85-99. https://doi.org/10.3233/jad-2012-111931

[9] Yushkevich PA, Wang H, Pluta J, Das SR, Craige C, Avants BB, et al. Nearly automatic segmentation of hippocampal subfields in in vivo focal T2-weighted MRI. Neuroimage 2010;53(4):1208-24. https://doi.org/10.1016/j.neuroimage.2010.06.040

[10] Amaral DG, Insausti R. The hippocampal formation. In: Paxinos G, editor The Human Nervous System, San Diego: Academic Press; 1990, p. 711-55.

[11] Duvernoy HM, Bourgouin P. The Human Hippocampus: Functional Anatomy, Vascularization, and Serial Sections with MRI. Berlin: Springer; 1998.

[12] Zhang Y, Brady M, Smith S. Segmentation of brain MR images through a hidden Markov random field model and the expectation-maximization algorithm. IEEE Trans Med Imaging 2001;20(1):45-57. https://doi.org/10.1109/42.906424
[13] Ekstrom A, Suthana N, Behnke E, Salamon N, Bookheimer S, Fried I. High-resolution depth electrode localization and imaging in patients with pharmacologically intractable epilepsy. J Neurosurg 2008;108(4):812-5. https://doi.org/10.3171/jns/2008/108/4/0812
[14] Suthana NA, Ekstrom AD, Moshirvaziri S, Knowlton B, Bookheimer SY. Human hippocampal CA1 involvement during allocentric encoding of spatial information. J Neurosci 2009;22:2231-7. https://doi.org/10.1523/JNEUROSCI.0621-09.2009
[15] Zeineh MM, Engel SA, Thompson PM, Bookheimer SY. Dynamics of the hippocampus during encoding and retrieval of face-name pairs. Science 2003;299(5606):577-80.
[16] Wechsler D. Wechsler Memory Scale, revised. New York: Psychological Corporation/ Harcourt Brace Jovanovich; 2005.
[17] Delis DC, Kramer JH, Kaplan E, Ober BA. California Verbal Learning Test. 2 ed. San Antonio, TX: Psychological Corporation; 2000.
[18] Meyers JE, Meyers KR, Rey. Complex Figure Test and recognition trial. Odessa, FL: Psychological Assessment Resources; 1995.
[19] Reitan RM. Trail Making Test: Manual for administration and scoring. Reitan Neuropsychology Laboratory; 1992.
[20] Yassa MA, Muftuler LT, Stark CE. Ultrahigh-resolution microstructural diffusion tensor imaging reveals perforant path degradation in aged humans in vivo. Proceedings of the national academy of sciences 2010;107(28):12687-91. https://doi.org/10.1073/pnas.1002113107